

Solar Type IIIb Radio Bursts as Tracers for Electron Density Fluctuations in the Corona

V. Mugundhan¹ · K. Hariharan² · R. Ramesh¹

Received: 14 May 2017 / Accepted: 25 September 2017
© Springer Science+Business Media B.V. 2017

Abstract We present an estimation of the electron density modulation index ($\frac{\delta N_e}{N_e}$) for the first time using solar type IIIb radio burst observations. The mean value of $\frac{\delta N_e}{N_e}$ is calculated to be $\approx 0.006 \pm 0.002$ over the heliocentric distance range $r \approx 1.6\text{--}2.2 R_\odot$. The estimated $\frac{\delta N_e}{N_e}$ shows a power law dependence on r with a power law index $\approx 0.31 \pm 0.10$. The wavenumber (k) spectrum for the electron density fluctuation ($\frac{\delta N_e}{N_e}$)² values shows a Kolmogorov-like behavior. Using $\frac{\delta N_e}{N_e}$ and the Kolmogorov turbulence index, we estimated the amplitude of density turbulence [$C_n^2(r)$] in the aforementioned range of r .

Keywords Corona, radio emission · Radio bursts, type III · Turbulence

1. Introduction

Inhomogeneities in the solar corona and the solar wind lead to turbulent density fluctuations. Study of the latter is important to understand the low values of observed radio brightness temperature of the “undisturbed” Sun and the angular broadening/location of compact solar radio sources (Aubier, Leblanc, and Boisshot, 1971; Bastian, 1994; Sastry, 1994; Thejappa and Kundu, 1994; Ramesh, 2000; Ramesh and Sastry, 2000; Ramesh, Subramanian, and Sastry, 2000; Kathiravan and Ramesh, 2004; Subramanian, 2004; Ramesh *et al.*, 2006, 2010b,

Combined Radio and Space-based Solar Observations: From Techniques to New Results
Guest Editors: Eduard Kontar and Alexander Nindos

✉ V. Mugundhan
mugundhan@iiap.res.in

✉ K. Hariharan
hara@ncra.tifr.res.in

✉ R. Ramesh
ramesh@iiap.res.in

¹ Indian Institute of Astrophysics, 2nd Block, Koramangala, Bangalore 560034, India

² NCRA-TIFR, Pune University Campus, Ganeshkhind P.O., Pune 411007, India

2012b; Subramanian and Cairns, 2011; Morosan *et al.*, 2014, 2015; Mercier and Chambe, 2015). Measurements of density fluctuations have been carried out over large heliocentric distances from $10 R_{\odot}$ up to $215 R_{\odot}$ (Bavassano and Bruno, 1995; Woo *et al.*, 1995; Ramesh, Kathiravan, and Sastry, 2001; Spangler, 2002; Tokumaru, Kojima, and Fujiki, 2012; Bisoï *et al.*, 2014; Sasikumar Raja *et al.*, 2016). However, such measurements below $10 R_{\odot}$ have not been possible to date due to various technical difficulties. Cairns *et al.* (2009) have suggested that observations of transient radio emission over the frequency range 30–300 MHz may be used to probe the density profile of the solar corona corresponding to $r \leq 2 R_{\odot}$.

Type III solar radio bursts are thought to be generated through plasma oscillations induced by energetic electron streams traveling along open magnetic field-lines (Ginzburg and Zhelezniakov, 1958; Sasikumar Raja and Ramesh, 2013; Reid and Ratcliffe, 2014). They appear as individual or a group (of 10 or more) fast drifting ($\delta f/\delta t \approx 100 \text{ MHz s}^{-1}$) enhanced features in the dynamic spectral records during the impulsive phase of flares (see *e.g.* Nindos *et al.*, 2011) with a duration of a few tens of seconds. Occasionally, however, they appear when there is little (*e.g.* Alissandrakis *et al.*, 2015) or no associated activity at other wavelengths.

At times, a chain of short duration narrow-band bursts have been observed to occur with an overall envelope having a drift rate similar to that of type III bursts and are called type IIIb bursts (Ellis and McCulloch, 1967; de La Noe and Boisshot, 1972). The spectral fragmentations within the type IIIb bursts are sometimes referred to as “striae” (de La Noe and Boisshot, 1972). Individual stria have been observed to have an average bandwidth and duration of $\approx 50 \text{ kHz}$ and $\approx 1.2 \text{ s}$, respectively. Takakura and Yousef (1975) have suggested that stria-like features in type IIIb bursts could be caused by density inhomogeneities along the path of the electron beams (Smith and de La Noe, 1976; Tun Beltran, Cutchin, and White, 2015). This has been verified subsequently through numerical modeling (Kontar, 2001; Li, Cairns, and Robinson, 2011a,b, 2012; Loi, Cairns, and Li, 2014). It has also been suggested by Loi, Cairns, and Li (2014) that the aforementioned properties of type IIIb bursts can be used to probe the density inhomogeneities in the solar corona and the solar wind.

To address the above, we present and analyze here the spectral observations of solar type IIIb radio bursts in the frequency range of 80–40 MHz from the Gauribidanur Radio Observatory located about 100 km north of Bangalore in India (Ramesh, 2011). The radio emission from the Sun corresponding to the above frequency interval typically originates in the distance range $r \approx 1.6\text{--}2.2 R_{\odot}$ in the solar corona.

2. Observations

The observations reported in this work were obtained with the *Gauribidanur Low Frequency Solar Spectrograph* (GLOSS; Ebenezer *et al.*, 2001, 2007; Kishore *et al.*, 2014) array. GLOSS is a phased-array of 8 log-periodic dipole antenna elements aligned along the north–south direction with the dipole arms along the east–west (EW) direction. The response pattern of the GLOSS in the EW direction is $\approx 90^\circ$ and this ensures that Sun is within the array field of view for 6 hours every day. A new digital *Fast Fourier Transform Spectrometer* (FFTS) configured on field-programmable gate array (FPGA) hardware was used as the back-end receiver for the GLOSS. The FFTS offers a spectral and temporal resolution of $\approx 24 \text{ kHz}$ and $\approx 5 \text{ ms}$, respectively. Further technical details of the FFTS back-end will be presented elsewhere (Hariharan, Mugundhan, and Ramesh, *in preparation*). Preliminary observations were performed with the GLOSS-FFTS system over the frequency range 40–80 MHz during the period July–October, 2016.

Figure 1 Type IIIb radio burst event recorded on 20 July 2016. The narrow-band features are striae which constitute the type IIIb burst.

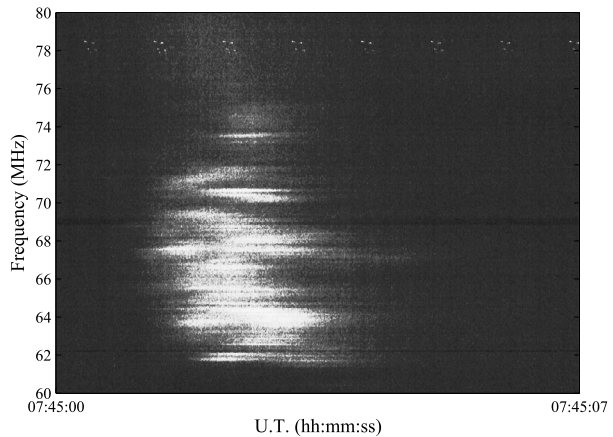
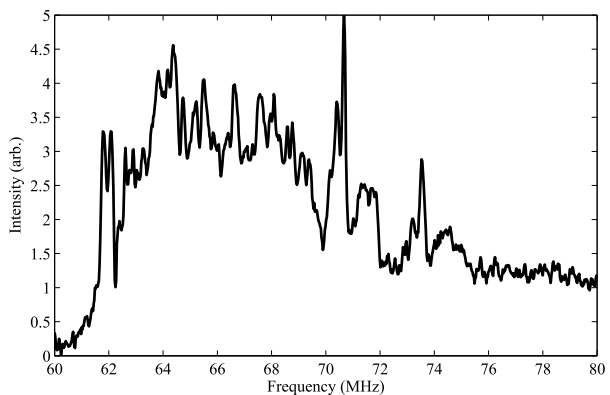


Figure 2 Spectral profile of the type IIIb radio burst event shown in Figure 1.



During the aforementioned observing period, type IIIb radio bursts were detected on four different days. Figure 1 shows a typical type IIIb radio burst observed with the GLOSS-FFTS on 20 July 2016, around 07:45 UT. The burst was not particularly associated with any flare at the time of occurrence,¹ although a SF class H α and a B6.6 class X-ray flare during 08:16–08:25 UT were reported from the active region AR 12565 located at the heliographic coordinates N01W34. We note that during the time of observation of the type IIIb bursts no particular flares at other wavelengths were reported. These bursts probably belong to the category of weak energy releases (Ramesh *et al.*, 2010a, 2013; Suresh *et al.*, 2017). A total of 19 type IIIb bursts were recorded with our instrument, each with a typical duration and bandwidth of ≈ 3 s and ≈ 15 MHz, respectively (refer to Table 1). Each of the type IIIb events were found to be composed of ≈ 15 –60 stria within the bandwidth of the burst. Figure 2 shows the instantaneous spectral profile of the type IIIb burst shown in Figure 1. The amplitude variations seen in the spectral-cut correspond to the striae within the type IIIb event. The individual stria were found to have a spectral width between 24–100 kHz with a duration of ≈ 1 s and did not show any significant drift in frequency. These are consistent with previously reported observations of type IIIb bursts (de La Noe and Boisshot, 1972; Krishan, Subramanian, and Sastry, 1980; Melnik *et al.*, 2009, 2011).

¹See <http://www.swpc.noaa.gov/>.

Table 1 List of type IIIb bursts recorded with FFTS.

Date	Time UT (hh:mm:ss)	Duration (s)	Frequency range (MHz)
20 July 2016	07:45:02	3	75–60
13 August 2016	05:37:14	3	68–54
	05:37:34	2	71–55
	05:38:04	4	72–54
	06:37:45	5	87–52
10 October 2016	08:58:02	2	80–55
	05:38:36	5	70–48
	06:15:21	4	65–48
12 October 2016	06:58:22	4	68–45
	06:03:57	3	59–47
	06:04:14	4	60–46
	06:05:11	2	58–47
	06:05:14	3	6–47
	06:05:40	3	62–48
	08:39:18	4	65–50
	08:39:23	2	70–55
08:39:25	3	68–53	
08:39:30	2	70–48	
08:40:39	3	58–43	

3. Analysis and Results

3.1. Estimation of $\frac{\delta N_e}{N_e}$

For the present work we have considered only the single individual stria bursts within the type IIIb events (see Table 1) for analysis in order to avoid ambiguities. The choice of the striae were constrained as follows: i) the striae are bright enough to be distinguishable from the smooth type III background; ii) the striae remain stationary in frequency with no noticeable frequency drift. From the spectral profile we marked and noted the upper (f_u), lower (f_l) and central (f_c) frequencies corresponding to the spectral width of the striae. The above values were then used to estimate $\frac{\delta N_e}{N_e}$ by applying Equations 1 and 2:

$$f_p = 8980\sqrt{N_e} \text{ Hz} \quad (1)$$

where N_e is in units of cm^{-3} , and

$$\frac{\delta N_e}{N_e} = \frac{f_u^2 - f_l^2}{f_c^2}. \quad (2)$$

The above analysis was carried out for each of the individual stria selected from all the type IIIb events reported in Table 1. Figure 3 shows the histogram distribution of the estimated values of $\frac{\delta N_e}{N_e}$ from all the type IIIb bursts listed in Table 1. It can be noted that the most frequent value of $\frac{\delta N_e}{N_e}$ is found to be $\approx 0.006 \pm 0.002$. This is consistent with the values of $\frac{\delta N_e}{N_e}$ at distances < 1 AU reported in the literature (Woo *et al.*, 1995; Bavassano and Bruno, 1995; Huddleston, Woo, and Neugebauer, 1995; Bisoi *et al.*, 2014).

Figure 3 A histogram of $\frac{\delta N_e}{N_e}$ obtained from type-IIIb events. The solid line is a Gaussian fit to the distribution.

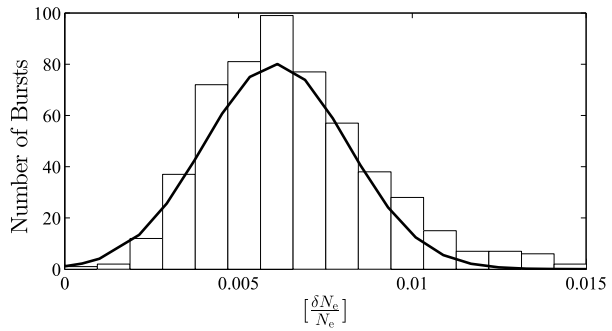
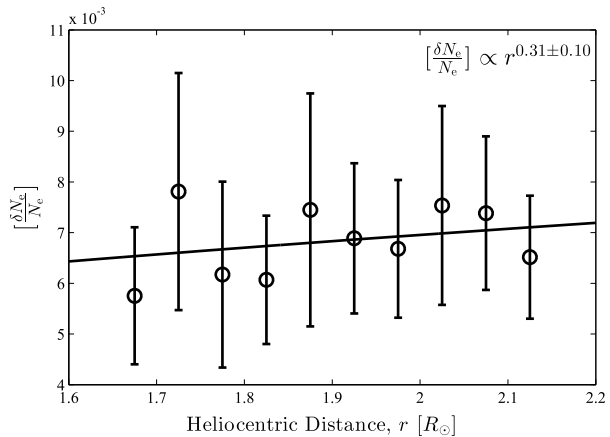


Figure 4 Distribution of mean $\frac{\delta N_e}{N_e}$ over $r \approx 1.6-2.2 R_\odot$. The solid line is a least-squares power law fit (refer to Table 2 for details). The error bars represent the spread in the data at the respective values of r .



We adopted the Baumbach–Allen electron density model (Baumbach, 1937; Allen, 1947) in order to study the radial dependence of $\frac{\delta N_e}{N_e}$. Assuming that the spectral fine structures in type IIIb bursts are due to density inhomogeneities along the path of the type III beam, we considered an enhancement factor of 10 similar to that considered in the simulation studies by Li, Cairns, and Robinson (2012) and Loi, Cairns, and Li (2014). Also, a $10\times$ Baumbach–Allen model represents a reasonable estimate of electron density enhancement in the corona during times of activity (Maxwell and Thompson, 1962; Stewart, 1976; Dryer and Maxwell, 1979; Ramesh *et al.*, 2005). Thus, when using the above model, our observing frequency range of 40–80 MHz then translates to $r \approx 1.6-2.2 R_\odot$. The study on the radial dependence of $\frac{\delta N_e}{N_e}$ was carried out for all the events on individual days of observation and also for the combined dataset from all four days, the results of which are summarized in Table 2.

Figure 4 shows the distribution of $\frac{\delta N_e}{N_e}$ values over heliocentric distance obtained from the combined data of all four days. A least-squares power law fit ($\propto r^\beta$) to the data indicates that $\frac{\delta N_e}{N_e}$ shows a weak variation with heliocentric distance, with an index $\beta \approx 0.31 \pm 0.10$. When estimated separately for each day, the obtained β is found to lie in the range of 0.28–0.40. Further, we find that mean value of $\frac{\delta N_e}{N_e}$ obtained from our measurements when combined with those obtained through other methods (*viz.* Interplanetary Scintillation (IPS), Radio Source occultation, *Very Long Baseline Interferometry* (VLBI) and spacecraft observations), also show a power law variation with $\beta \approx 0.33$ over $r = 1.5-215 R_\odot$ (refer to Figure 5). Reid and Kontar (2010) also predicted similar variation of $\frac{\delta N_e}{N_e}$ ($\propto r^{0.25}$) up to 1 AU for

Figure 5 Distribution of Density modulation index ($\frac{\delta N_e}{N_e}$) over the heliocentric distance range from $\approx 1.5 - 215 R_\odot$ (1 AU). The axes are in log-log scale. The error bars represent the spread in the data at the respective values of r . The solid line represents a least-square power law fit to the data, with a power law index of ≈ 0.33 .

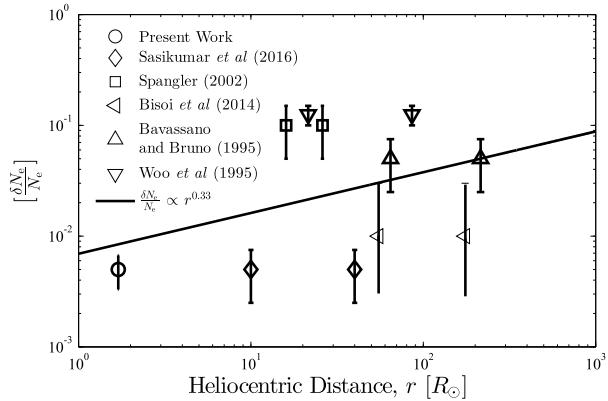


Table 2 Summary of analysis.

Date	$\frac{\delta N_e}{N_e}$ (%)	Heliocentric distance (r) (R_\odot)	Power law index (β)
20 July 2016	0.5 ± 0.11	1.6–2.0	0.29 ± 0.13
13 August 2016	0.6 ± 0.19	1.6–2.1	0.40 ± 0.15
10 October 2016	0.5 ± 0.12	1.7–2.2	0.31 ± 0.10
12 October 2016	0.6 ± 0.23	1.7–2.2	0.28 ± 0.11
Overall	0.6 ± 0.20	1.6–2.2	0.31 ± 0.10

transport of type III electrons. This shows that the $\frac{\delta N_e}{N_e}$ ratio obtained here is consistent with previously reported values and follows the same trend in the inner corona as well.

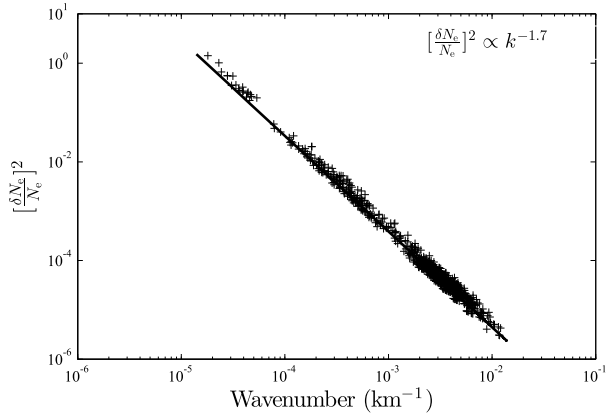
3.2. Nature of Density Fluctuations

It has been suggested that the solar corona and solar wind follow a Kolmogorov-like power-law spectrum with wavenumber $k = 2\pi/l$, where l is the scale size involved in the turbulence cascade (Marsch, 1991; Goldstein, Roberts, and Matthaeus, 1995; Cranmer, 2007). Since we carried out spectral observations, the largest and smallest measurable scales depend on the observation bandwidth and frequency resolution, respectively. The scales are estimated using the density model assumed in the previous section. Since the spectral enhancements in the type IIIb burst could be due to local density inhomogeneities, the bandwidth of the striae at different frequencies correspond to the turbulence scale there (Loi, Cairns, and Li, 2014). Figure 6 shows the $(\frac{\delta N_e}{N_e})^2$ spectrum in log scale, where the small and intermediate scales correspond to the spectral width of the individual stria and their fluctuating background, respectively while the large scales correspond to the overall spectral extent of the type IIIb burst.

A fit to the data shows that the spectrum has an index $\alpha \approx -1.70 \pm 0.02$. This is in close agreement with the one-dimensional Kolmogorov spectral index [$\propto k^{-5/3}$] (Reid and Kontar, 2010; Loi, Cairns, and Li, 2014). The minimum scale length estimated from our data corresponds to $l_{\min} \approx 520$ km. But even after reaching this scale, there is no evidence of spectral flattening which is expected beyond the inner scale. This suggests that the inner scale² (l_i) could be smaller than the minimum scale obtained from this dataset. Note that

²The scale beyond which turbulence cascade energy begins to dissipate.

Figure 6 Spectrum of $(\frac{\delta N_e}{N_e})^2$ fluctuations. Both axes are plotted in log scale.



flattening of the spectrum ($\propto k^{-1.1}$) at distances $\leq 20 R_\odot$ has been observed (Woo and Armstrong, 1979); The former has been reported to set in at shorter scales ($\approx 3 - 300$ km), shifting to larger k sunward (Coles *et al.*, 1991; Imamura *et al.*, 2005; Mullan, 1990).

3.3. Determination of $C_n^2(r)$

As a corollary, we used the estimated $\frac{\delta N_e}{N_e}$ and α to calculate the amplitude of density fluctuations, $C_n^2(r)$. To date, estimation of $C_n^2(r)$ has only been performed for $r = 10 - 60 R_\odot$, using *in situ* spacecraft and VLBI observations (refer to Section 1). Sasikumar Raja *et al.* (2016) used data from the occultation of the radio source 3C144 by the solar corona to obtain $C_n^2(r)$ for $r = 10 - 45 R_\odot$. They found a solar-cycle dependent power-law variation of $C_n^2(r)$ with r .

The relation between $(\frac{\delta N_e}{N_e})^2$, α and $C_n^2(r)$, for a one-dimensional turbulence spectrum at the inner scale usually is (Sasikumar Raja *et al.*, 2016; Subramanian and Cairns, 2011 and the references therein):

$$C_n^2(r) \propto \frac{[\frac{\delta N_e}{N_e}]^2 N_e^2}{4\pi k_i^{2-\alpha} e^{-1}}, \tag{3}$$

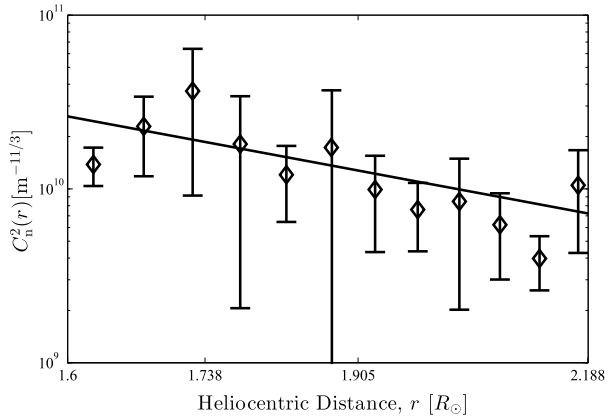
where the wavenumber at the inner scale (l_i) is $k_i = \frac{2\pi}{l_i}$. Note that for a three-dimensional turbulence spectrum k_i is raised to $3-\alpha$.

There has been considerable debate as to what the smallest scale is that is present in the corona and the solar wind (Mullan, 1990). Sasikumar Raja *et al.* (2016) have shown that scales of the order of 1.6 km exist at $r < 10 R_\odot$. In view of recent *in situ* spacecraft and IPS observations (Bale *et al.*, 2005; Alexandrova *et al.*, 2009, 2012; Bisoï *et al.*, 2014), it has been suggested that dissipation could occur down to proton and electron gyro-radii scales (ρ_p) (Chen *et al.*, 2014). The proton gyro-radius (ρ_p) is given by

$$\rho_p(r) = 102\sqrt{\mu T_i} B(r)^{-1} \quad [\text{cm}], \tag{4}$$

where μ is the ratio of the mass of ions to that of protons, which is ≈ 1 , and where T_i is the proton temperature in eV, and $B(r)$ is the coronal magnetic field, which can be modeled as $B(r) = 0.5(r - 1)^{-1.5}$ [G] with r in units of R_\odot (Dulk and McLean, 1978; Ramesh, Kathiravan, and Sastry, 2010; Ramesh, Kathiravan, and Narayanan, 2011).

Figure 7 Log–log plot of $C_n^2(r)$ with r , for a spectrum with $\alpha \approx -1.7$ and inner scale as electron gyro-radius. The *solid line* is a power law fit of the form Ar^γ . The fitted values are $A = 1.8 \pm 1.0 \times 10^{11} \text{ m}^{-11/3}$ and $\gamma = -4.11 \pm 1.75$. The *error bars* represent the spread in the data at the respective values of r .



The electron gyro-radius (ρ_e) is

$$\rho_e = 2.38\sqrt{T_e B(r)^{-1}} \quad [\text{cm}]. \tag{5}$$

In this work, we consider both electron and proton gyro-radii as the inner scale for $C_n^2(r)$ estimation. We used Equation 3 to obtain the $C_n^2(r)$ values corresponding to $\frac{\delta N_e}{N_e}$ using α estimated earlier in this paper (see Section 3.2) for both inner scale estimates. The $C_n^2(r)$ calculated was binned to different solar radii and its scatter with respect to r was obtained. A least-squares power law of the form Ar^γ was fit to the data obtained for both inner scale considerations. We show a representative scatter of the behavior of $C_n^2(r)$ against r , considering $l_i = \rho_e$ in Figure 7. A similar fit with $l_i = \rho_p$ yielded the following fit parameters: $A \approx 4.79 \pm 1.50 \times 10^{11} \text{ m}^{-11/3}$ and $\gamma \approx -4.09 \pm 2.00$. However, the $C_n^2(r)$ estimates have to be treated with caution as these depend strongly on l_i , which is not yet precisely known.

4. Conclusion

We report the first estimate $\frac{\delta N_e}{N_e}$ and $C_n^2(r)$ for $r = 1.6\text{--}2.2 R_\odot$ from the observations of type IIIb solar radio bursts. $\frac{\delta N_e}{N_e}$ varies with r as a power law with index $\beta \approx 0.33$. Note that previous estimates of $\frac{\delta N_e}{N_e}$ through techniques like IPS, Radio Source occultation, VLBI and *in situ* spacecraft measurements were limited to $r \geq 10 R_\odot$ (Woo *et al.*, 1995; Bavassano and Bruno, 1995; Ramesh, Kathiravan, and Sastry, 2001; Spangler, 2002; Bisoi *et al.*, 2014; Sasikumar Raja *et al.*, 2016). It has been suggested by several authors (Takakura and Yousef, 1975; Smith and de La Noe, 1976; de La Noe and Boisshot, 1972; Tun Beltran, Cutchin, and White, 2015) that striations in type IIIb radio burst emission can be due to electron density variations along the path the electron beams causing the type III bursts. Subsequent numerical modeling has shown that stria-like fine-structure emissions can indeed arise from density or temperature inhomogeneities along the path of the exciter and thus can be effective probes of the same (Kontar, 2001; Li, Cairns, and Robinson, 2011a,b, 2012; Loi, Cairns, and Li, 2014). We use the values of $(\frac{\delta N_e}{N_e})^2$ obtained from the data and determine that the density modulation index follows a Kolmogorov-like spectrum ($\propto k^{-1.7}$) for the range of values of r examined in this work.

As a corollary, we use the obtained values of $(\frac{\delta N_e}{N_e})^2$ and α to estimate the behavior of $C_n^2(r)$ with r . It is found that the former shows a power law variation radially with an index ≈ -4.2 .

The results obtained in the present work are consistent with those obtained using other techniques *viz.* IPS, VLBI and occultation experiments. Studies like the one presented here are useful to understand scattering due to density fluctuations in the solar corona, and the spatial extent of the smallest observed compact sources there (Ramesh, Subramanian, and Sastry, 1999; Ramesh and Sastry, 2000; Ramesh and Ebenezer, 2001; Mercier *et al.*, 2006, 2015; Kathiravan *et al.*, 2011; Ramesh *et al.*, 2012a; Mugundhan *et al.*, 2016). We conclude by stating that observations of fine-structure/fragmented radio emission (Thejappa, Zlobec, and MacDowall, 2003; Pohjolainen, Pomoell, and Vainio, 2008; Tun Beltran, Cutchin, and White, 2015) with high spectro-temporal resolution (Hariharan *et al.*, 2016) can be used as a proxy for density turbulence measurements in the solar corona, particularly in the range $r < 10 R_\odot$ which is presently unavailable.

Acknowledgements We thank the staff of the Gauribidanur Observatory for their help in observations, and maintenance of the antenna, receiver systems there. VM would like to thank Dr. C. Kathiravan and Ms. Anshu Kumari for their contributions towards thoroughly proof-reading the manuscript and providing valuable suggestions. We acknowledge the referee for his/her comments and suggestions which helped us in bringing out the results more clearly.

Disclosure of Potential Conflicts of interest We declare that there are no conflicts of interest for the work presented here.

References

- Alexandrova, O., Saur, J., Lacombe, C., Mangeney, A., Mitchell, J., Schwartz, S.J., Robert, P.: 2009, Universality of solar-wind turbulent spectrum from MHD to electron scales. *Phys. Rev. Lett.* **103**(16), 165003. [DOI](#). [ADS](#).
- Alexandrova, O., Lacombe, C., Mangeney, A., Grappin, R., Maksimovic, M.: 2012, Solar wind turbulent spectrum at plasma kinetic scales. *Astrophys. J.* **760**, 121. [DOI](#). [ADS](#).
- Alissandrakis, C.E., Nindos, A., Patsourakos, S., Kontogeorgos, A., Tsiatsipis, P.: 2015, A tiny event producing an interplanetary type III burst. *Astron. Astrophys.* **582**, A52. [DOI](#). [ADS](#).
- Allen, C.W.: 1947, Interpretation of electron densities from corona brightness. *Mon. Not. Roy. Astron. Soc.* **107**, 426. [DOI](#). [ADS](#).
- Aubier, M., Leblanc, Y., Boisshot, A.: 1971, Observations of the quiet Sun at decameter wavelengths – Effects of scattering on the brightness distribution. *Astron. Astrophys.* **12**, 435. [ADS](#).
- Bale, S.D., Kellogg, P.J., Mozer, F.S., Horbury, T.S., Reme, H.: 2005, Measurement of the electric fluctuation spectrum of magnetohydrodynamic turbulence. *Phys. Rev. Lett.* **94**(21), 215002. [DOI](#). [ADS](#).
- Bastian, T.S.: 1994, Angular scattering of solar radio emission by coronal turbulence. *Astrophys. J.* **426**, 774. [DOI](#). [ADS](#).
- Baumbach, S.: 1937, Strahlung, ergiebigkeit und elektronendichte der sonnenkorona. *Astron. Nachr.* **263**(6), 121. [DOI](#).
- Bavassano, B., Bruno, R.: 1995, Density fluctuations and turbulent Mach numbers in the inner solar wind. *J. Geophys. Res.* **100**, 9475. [DOI](#). [ADS](#).
- Bisoi, S.K., Janardhan, P., Ingale, M., Subramanian, P., Ananthkrishnan, S., Tokumar, M., Fujiki, K.: 2014, A study of density modulation index in the inner heliospheric solar wind during Solar Cycle 23. *Astrophys. J.* **795**, 69. [DOI](#). [ADS](#).
- Cairns, I.H., Lobzin, V.V., Warmuth, A., Li, B., Robinson, P.A., Mann, G.: 2009, Direct radio probing and interpretation of the Sun's plasma density profile. *Astrophys. J. Lett.* **706**, L265. [DOI](#). [ADS](#).
- Chen, C.H.K., Leung, L., Boldyrev, S., Maruca, B.A., Bale, S.D.: 2014, Ion-scale spectral break of solar wind turbulence at high and low beta. *Geophys. Res. Lett.* **41**(22), 8081. [DOI](#).
- Coles, W., Liu, W., Harmon, J., Martin, C.: 1991, The solar wind density spectrum near the sun: Results from voyager radio measurements. *J. Geophys. Res. Space Phys.* **96**(A2), 1745.

- Cranmer, S.R.: 2007, Turbulence in the solar corona. In: Shaikh, D., Zank, G.P. (eds.) *Turbulence and Non-linear Processes in Astrophysical Plasmas*, American Institute of Physics Conference Series **932**, 327. DOI. ADS.
- de La Noe, J., Boisshot, A.: 1972, The type III B burst. *Astron. Astrophys.* **20**, 55. ADS.
- Dryer, M., Maxwell, A.: 1979, Radio data and a theoretical model for the fast-mode MHD shock wave generated by the solar flare of 1973 September 5, 18:26 UT. *Astrophys. J.* **231**, 945. DOI. ADS.
- Dulk, G.A., McLean, D.J.: 1978, Coronal magnetic fields. *Solar Phys.* **57**, 279. DOI. ADS.
- Ebenezer, E., Ramesh, R., Subramanian, K.R., SundaraRajan, M.S., Sastry, C.V.: 2001, A new digital spectrograph for observations of radio burst emission from the Sun. *Astron. Astrophys.* **367**, 1112. DOI. ADS.
- Ebenezer, E., Subramanian, K.R., Ramesh, R., Sundararajan, M.S., Kathiravan, C.: 2007, Gauribidanur Radio Array Solar Spectrograph (GRASS). *Bull. Astron. Soc. India* **35**, 111. ADS.
- Ellis, G.R.A., McCulloch, P.M.: 1967, Frequency splitting of solar radio bursts. *Aust. J. Phys.* **20**, 583. DOI. ADS.
- Ginzburg, V.L., Zhelezniakov, V.V.: 1958, On the possible mechanisms of sporadic solar radio emission (radiation in an isotropic plasma). *Soviet Astron.* **2**, 653. ADS.
- Goldstein, M.L., Roberts, D., Matthaeus, W.: 1995, Magnetohydrodynamic turbulence in the solar wind. *Annu. Rev. Astron. Astrophys.* **33**(1), 283.
- Hariharan, K., Mugundhan, V., Ramesh, R.: In preparation. Digital spectrometers for solar radio astronomy.
- Hariharan, K., Ramesh, R., Kathiravan, C., Abhilash, H.N., Rajalingam, M.: 2016, High dynamic range observations of solar coronal transients at low radio frequencies with a spectro-correlator. *Astrophys. J. Suppl.* **222**, 21. DOI. ADS.
- Huddleston, D.E., Woo, R., Neugebauer, M.: 1995, Density fluctuations in different types of solar wind flow at 1 AU and comparison with results from Doppler scintillation measurement near the Sun. *J. Geophys. Res.* **100**, 19951. DOI. ADS.
- Imamura, T., Noguchi, K., Nabatov, A., Oyama, K.-I., Yamamoto, Z., Tokumaru, M.: 2005, Phase scintillation observation during coronal sounding experiments with NOZOMI spacecraft. *Astron. Astrophys.* **439**, 1165. DOI. ADS.
- Kathiravan, C., Ramesh, R.: 2004, Estimation of the three-dimensional space speed of a coronal mass ejection using metric radio data. *Astrophys. J.* **610**, 532. DOI. ADS.
- Kathiravan, C., Ramesh, R., Barve, I.V., Rajalingam, M.: 2011, Radio observations of the solar corona during an eclipse. *Astrophys. J.* **730**, 91. DOI. ADS.
- Kishore, P., Kathiravan, C., Ramesh, R., Rajalingam, M., Barve, I.V.: 2014, Gauribidanur low-frequency solar spectrograph. *Solar Phys.* **289**, 3995. DOI. ADS.
- Kontar, E.P.: 2001, Dynamics of electron beams in the solar corona plasma with density fluctuations. *Astron. Astrophys.* **375**, 629. DOI. ADS.
- Krishan, V., Subramanian, K.R., Sastry, C.V.: 1980, Observations and interpretation of solar decameter type IIIb radio bursts. *Solar Phys.* **66**, 347. DOI. ADS.
- Li, B., Cairns, I.H., Robinson, P.A.: 2011a, Effects of spatial variations in coronal electron and ion temperatures on type III bursts. II. Variations in ion temperature. *Astrophys. J.* **730**, 21. DOI. ADS.
- Li, B., Cairns, I.H., Robinson, P.A.: 2011b, Effects of spatial variations in coronal temperatures on type III bursts. I. Variations in electron temperature. *Astrophys. J.* **730**, 20. DOI. ADS.
- Li, B., Cairns, I.H., Robinson, P.A.: 2012, Frequency fine structures of type III bursts due to localized medium-scale density structures along paths of type III beams. *Solar Phys.* **279**, 173. DOI. ADS.
- Loi, S.T., Cairns, I.H., Li, B.: 2014, Production of fine structures in type III solar radio bursts due to turbulent density profiles. *Astrophys. J.* **790**, 67. DOI. ADS.
- Marsch, E.: 1991, Turbulence in the solar wind. In: Klare, G. (ed.) *Reviews in Modern Astronomy, Reviews in Modern Astronomy* **4**, 145. DOI. ADS.
- Maxwell, A., Thompson, A.R.: 1962, Spectral observations of solar radio bursts. II. Slow-drift bursts and coronal streamers. *Astrophys. J.* **135**, 138. DOI. ADS.
- Melnik, V.N., Rucker, H.O., Konvalenko, A.A., Dorovskyy, V.V., Tan, S.: 2011, Decameter IIIb-III pairs. In: *EPSC-DPS Joint Meeting 2011*, 796. ADS.
- Melnik, V., Rucker, H., Konvalenko, A., Abranin, E., Dorovskyy, V., Boiko, A., Lecacheux, A.: 2009, Observation of powerful solar type III bursts at frequencies 10–30 MHz. In: *European Planetary Science Congress 2009*, 421. ADS.
- Mercier, C., Chambe, G.: 2015, Electron density and temperature in the solar corona from multifrequency radio imaging. *Astron. Astrophys.* **583**, A101. DOI. ADS.
- Mercier, C., Subramanian, P., Kerdraon, A., Pick, M., Ananthkrishnan, S., Janardhan, P.: 2006, Combining visibilities from the giant meterwave radio telescope and the Nancay radio heliograph. High dynamic range snapshot images of the solar corona at 327 MHz. *Astron. Astrophys.* **447**, 1189. DOI. ADS.

- Mercier, C., Subramanian, P., Chambe, G., Janardhan, P.: 2015, The structure of solar radio noise storms. *Astron. Astrophys.* **576**, A136. DOI. ADS.
- Morosan, D.E., Gallagher, P.T., Zucca, P., Fallows, R., Carley, E., Mann, G., Bisi, M., Kerdraon, A., Konovalenko, A., MacKinnon, A., et al.: 2014, LOFAR tied-array imaging of type III solar radio bursts. *Astron. Astrophys.* **568**, A67.
- Morosan, D., Gallagher, P., Zucca, P., O'flannagain, A., Fallows, R., Reid, H., Magdalenic, J., Mann, G., Bisi, M., Kerdraon, A., et al.: 2015, LOFAR tied-array imaging and spectroscopy of solar S bursts. *Astron. Astrophys.* **580**, A65.
- Mugundhan, V., Ramesh, R., Barve, I.V., Kathiravan, C., Gireesh, G.V.S., Kharb, P., Misra, A.: 2016, Low-frequency radio observations of the solar corona with arcminute angular resolution: Implications for coronal turbulence and weak energy releases. *Astrophys. J.* **831**, 154. DOI. ADS.
- Mullan, D.J.: 1990, Sources of the solar wind – What are the smallest-scale structures? *Astron. Astrophys.* **232**, 520. ADS.
- Nindos, A., Alissandrakis, C.E., Hillaris, A., Preka-Papadema, P.: 2011, On the relationship of shock waves to flares and coronal mass ejections. *Astron. Astrophys.* **531**, A31. DOI. ADS.
- Pohjolainen, S., Pomoell, J., Vainio, R.: 2008, CME liftoff with high-frequency fragmented type II burst emission. *Astron. Astrophys.* **490**, 357. DOI. ADS.
- Ramesh, R.: 2000, Low frequency radio emission from the 'quiet Sun'. *J. Astrophys. Astron.* **21**, 237. DOI. ADS.
- Ramesh, R.: 2011, Low frequency solar radio astronomy at the Indian Institute of Astrophysics (IIA). In: *Astronomical Society of India Conference Series, Astronomical Society of India Conference Series 2*. ADS.
- Ramesh, R., Ebenezer, E.: 2001, Decameter wavelength observations of an absorption burst from the Sun and its association with an X2.0/3B flare and the onset of a "Halo" coronal mass ejection. *Astrophys. J. Lett.* **558**, L141. DOI. ADS.
- Ramesh, R., Sastry, C.V.: 2000, Radio observations of a coronal mass ejection induced depletion in the outer solar corona. *Astron. Astrophys.* **358**, 749. ADS.
- Ramesh, R., Kathiravan, C., Narayanan, A.S.: 2011, Low-frequency observations of polarized emission from long-lived non-thermal radio sources in the solar corona. *Astrophys. J.* **734**, 39. DOI. ADS.
- Ramesh, R., Kathiravan, C., Sastry, C.V.: 2001, Low-frequency radio observations of the angular broadening of the Crab nebula due to a coronal mass ejection. *Astrophys. J. Lett.* **548**, L229. DOI. ADS.
- Ramesh, R., Kathiravan, C., Sastry, C.V.: 2010, Estimation of magnetic field in the solar coronal streamers through low frequency radio observations. *Astrophys. J.* **711**, 1029. DOI. ADS.
- Ramesh, R., Subramanian, K.R., Sastry, C.V.: 1999, Eclipse observations of compact sources in the outer solar corona. *Solar Phys.* **185**, 77. DOI. ADS.
- Ramesh, R., Subramanian, K.R., Sastry, C.V.: 2000, Estimation of the altitude and electron density of a discrete source in the outer solar corona through low frequency radio observations. *Astrophys. Lett. Commun.* **40**, 93. ADS.
- Ramesh, R., Narayanan, A.S., Kathiravan, C., Sastry, C.V., Shankar, N.U.: 2005, An estimation of the plasma parameters in the solar corona using quasi-periodic metric type III radio burst emission. *Astron. Astrophys.* **431**, 353. DOI. ADS.
- Ramesh, R., Nataraj, H.S., Kathiravan, C., Sastry, C.V.: 2006, The equatorial background solar corona during solar minimum. *Astrophys. J.* **648**, 707. DOI. ADS.
- Ramesh, R., Kathiravan, C., Barve, I.V., Beeharry, G.K., Rajasekara, G.N.: 2010a, Radio observations of weak energy releases in the solar corona. *Astrophys. J. Lett.* **719**, L41. DOI. ADS.
- Ramesh, R., Kathiravan, C., Kartha, S.S., Gopalswamy, N.: 2010b, Radioheliograph observations of metric type II bursts and the kinematics of coronal mass ejections. *Astrophys. J.* **712**, 188. DOI. ADS.
- Ramesh, R., Kathiravan, C., Barve, I.V., Rajalingam, M.: 2012a, High angular resolution radio observations of a coronal mass ejection source region at low frequencies during a solar eclipse. *Astrophys. J.* **744**, 165. DOI. ADS.
- Ramesh, R., Lakshmi, M.A., Kathiravan, C., Gopalswamy, N., Umapathy, S.: 2012b, The location of solar metric type II radio bursts with respect to the associated coronal mass ejections. *Astrophys. J.* **752**, 107. DOI. ADS.
- Ramesh, R., Sasikumar Raja, K., Kathiravan, C., Narayanan, A.S.: 2013, Low-frequency radio observations of picoflare category energy releases in the solar atmosphere. *Astrophys. J.* **762**, 89. DOI. ADS.
- Reid, H.A.S., Kontar, E.P.: 2010, Solar wind density turbulence and solar flare electron transport from the Sun to the Earth. *Astrophys. J.* **721**, 864. DOI. ADS.
- Reid, H.A.S., Ratcliffe, H.: 2014, A review of solar type III radio bursts. *Res. Astron. Astrophys.* **14**, 773. DOI. ADS.
- Sasikumar Raja, K., Ramesh, R.: 2013, Low-frequency observations of transient quasi-periodic radio emission from the solar atmosphere. *Astrophys. J.* **775**, 38. DOI. ADS.

- Sasikumar Raja, K., Ingale, M., Ramesh, R., Subramanian, P., Manoharan, P.K., Janardhan, P.: 2016, Amplitude of solar wind density turbulence from 10 to 45 R_{\odot} . *J. Geophys. Res. Space Phys.* **121**, 11. DOI. ADS.
- Sastry, C.V.: 1994, Observations of the continuum radio emission from the undisturbed Sun at a wavelength of 8.7 meters. *Solar Phys.* **150**, 285. DOI. ADS.
- Smith, R.A., de La Noe, J.: 1976, Theory of type IIIb solar radio bursts. *Astrophys. J.* **207**, 605. DOI. ADS.
- Spangler, S.R.: 2002, The amplitude of magnetohydrodynamic turbulence in the inner solar wind. *Astrophys. J.* **576**, 997. DOI. ADS.
- Stewart, R.T.: 1976, Source heights of metre wavelength bursts of spectral types I and III. *Solar Phys.* **50**, 437. DOI. ADS.
- Subramanian, K.R.: 2004, Brightness temperature and size of the quiet Sun at 34.5 MHz. *Astron. Astrophys.* **426**, 329. DOI. ADS.
- Subramanian, P., Cairns, I.: 2011, Constraints on coronal turbulence models from source sizes of noise storms at 327 MHz. *J. Geophys. Res. Space Phys.* **116**(A3), A03104. DOI.
- Suresh, A., Sharma, R., Oberoi, D., Das, S.B., Pankratius, V., Timar, B., Lonsdale, C.J., Bowman, J.D., *et al.*: 2017, Wavelet-based characterization of small-scale solar emission features at low radio frequencies. *Astrophys. J.* **843**, 19. DOI. ADS.
- Takakura, T., Yousef, S.: 1975, Type IIIb radio bursts – 80 MHz source position and theoretical model. *Solar Phys.* **40**, 421. DOI. ADS.
- Thejappa, G., Kundu, M.R.: 1994, The effects of large- and small-scale density structures on the radio from coronal streamers. *Solar Phys.* **149**, 31. DOI. ADS.
- Thejappa, G., Zlobec, P., MacDowall, R.J.: 2003, Polarization and fragmentation of solar type II radio bursts. *Astrophys. J.* **592**, 1234. DOI. ADS.
- Tokumaru, M., Kojima, M., Fujiki, K.: 2012, Long-term evolution in the global distribution of solar wind speed and density fluctuations during 1997–2009. *J. Geophys. Res. Space Phys.* **117**, A06108. DOI. ADS.
- Tun Beltran, S.D., Cutchin, S., White, S.: 2015, A new look at type-III bursts and their use as coronal diagnostics. *Solar Phys.* **290**, 2423. DOI. ADS.
- Woo, R., Armstrong, J.W.: 1979, Spacecraft radio scattering observations of the power spectrum of electron density fluctuations in the solar wind. *J. Geophys. Res. Space Phys.* **84**(A12), 7288. DOI.
- Woo, R., Armstrong, J.W., Bird, M.K., Patzold, M.: 1995, Variation of fractional electron density fluctuations inside 40 R_0 observed by ULYSSES ranging measurements. *Geophys. Res. Lett.* **22**, 329. DOI. ADS.